Small interfering RNA targeting ILK inhibits EMT in human peritoneal mesothelial cells through phosphorylation of GSK-3β

LINGRONG LUO[1], HONG LIU[1], ZHENG DONG[2], LIN SUN[1], YOUMING PENG[1] and FUYOU LIU[1]

[1]Department of Nephrology, Second Xiangya Hospital, Central South University, Changsha, Hunan 410011, P.R. China; [2]Department of Cellular Biology and Anatomy, Medical College of Georgia, Augusta, GA 30912, USA

Received July 17, 2013; Accepted March 11, 2014

DOI: 10.3892/mmr.2014.2162

Abstract. Emerging evidence has suggested that human peritoneal mesothelial cells (HPMCs) undergo epithelial-mesenchymal transition (EMT) in peritoneal fibrosis. The molecular mechanisms underlying peritoneal fibrosis and the key molecules involved are not yet fully elucidated. In order to enhance the understanding of peritoneal fibrosis, the present study investigated the roles of integrin-linked kinase (ILK) and glycogen synthase kinase 3β (GSK-3β) in high glucose-induced phenotypic alterations of HPMCs. It was observed that HPMCs exhibited a cobblestone morphology under normal glucose conditions, whereas under high glucose conditions they had a spindle morphology. Additionally, under high glucose conditions it was found that E-cadherin expression was decreased and vimentin expression was increased in HPMCs, suggesting HPMCs underwent EMT. ILK expression in high glucose conditions was also increased in a dose- and time-dependent manner. The role of ILK in the induction of EMT in HPMCs was further investigated using small interfering RNA (siRNA). Following knockdown of ILK gene expression by siRNA, low vimentin expression as well as high E-cadherin expression were observed, suggesting that EMT was inhibited. ILK-knockdown also inhibited phosphorylation of GSK-3β. These results indicate that ILK-knockdown inhibits EMT of HPMCs through inhibition of GSK-3β phosphorylation. These findings suggest that ILK may be used as a novel diagnostic and therapeutic target for HPMC fibrosis in the future.

Correspondence to: Dr Fuyou Liu, Department of Nephrology, Second Xiangya Hospital, Central South University, 139 Renmin Middle Road, Changsha, Hunan 410011, P.R. China
E-mail: xysblt@163.com

Key words: integrin-linked kinase, glycogen synthase kinase 3β, human peritoneal mesothelial cells, epithelial-mesenchymal transition, peritoneal dialysis

Introduction

In the past decades peritoneal dialysis (PD) has become an established alternative therapy to hemodialysis for the treatment of end-stage renal disease. The number of patients who receiving PD therapy has increased progressively worldwide, particularly in Asian countries. However, peritoneal fibrosis is an inevitable consequence of PD and is one of the most important causes of ultrafiltration failure (1-3). Previous studies have found that the epithelial-mesenchymal transition (EMT) of human peritoneal mesothelial cells (HPMCs) is an early event during PD and is associated with high peritoneal transport. HPMC EMT is a key process leading to peritoneal fibrosis and function deterioration (4-7). During dialysis, the peritoneum is exposed to continuous inflammatory stimuli, including hyperosmotic, hyperglycemic and acidic dialysis solutions, as well as peritonitis and hemoperitoneum. These factors may cause acute and chronic inflammation of the peritoneum, and may progressively lead to fibrosis, angiogenesis and hyalinizing vasculopathy (8-10). The mechanism by which high glucose levels elicit EMT has been a major focus of current research on fibrosis.

Integrin-linked kinase (ILK) is a protein discovered in 1996 using a yeast two-hybrid screen in which the cytoplasmic tail of β1 integrin was used as the bait (11). ILK consists of an N-terminal domain that contains four ankyrin repeats, a central pleckstrin homology-like domain and a C-terminal kinase domain (12). ILK is a protein that has an important role in extracellular matrix (ECM)-mediated signaling. It is a key molecule in the mediation of several biological functions, including cell-matrix interactions, angiogenesis and invasion. It is also involved in the EMT of podocytes and renal interstitial fibrosis (13,14). Aberrant regulation of ILK is implicated in the pathogenesis of various proteinuric kidney diseases, including diabetic nephropathy, congenital nephritic syndrome and experimental models of glomerular disease (15-17). In addition, ILK has been shown to be an important intracellular mediator that controls EMT in tubular epithelial cells (18). Furthermore, it has been proposed that ILK regulates the phosphorylation of Akt at Ser 473 and the phosphorylation of glycogen synthase kinase 3β (GSK-3β) in various cell types (19,20), which suggests that ILK may have a role in EMT.

In the present study, a preliminary experiment revealed that there was a large and complex network of molecular

signals in EMT. Among these key molecules, ILK, a downstream factor of transforming growth factor β1 (TGF-β1), participates in multiple signaling pathways, including the integrin, TGF-β1/Sma- and Mad-related protein (Smad), mitogen-activated protein kinases (MAPK), connective tissue growth factor (CTGF), phosphoinositide 3-kinase (PI3K)/AKT and extracellular signal-regulated kinase 1/2 (ERK1/2) pathways (21-24). To date, to the best of our knowledge, there have been no published data on ILK expression patterns in HPMCs. Therefore, in this study, the role of ILK in the regulation of HPMC EMT induced by high glucose conditions was investigated.

Materials and methods

Cell culture. HPMCs were provided by Dr Pierre Ronco (Tenon Hospital, Paris, France). The isolation, primary culture and immortalization of HPMC cell line were performed as previously described (25,26). The cell line was established following infection of a fully characterized primary culture of human peritoneal mesothelial cells with an amphotropic recombinant retrovirus that encodes SV40 large-T Ag under the control of the Moloney virus long terminal repeat and resistance to the antibiotic G418. Briefly, cells were cultured in low-glucose Dulbecco's modified Eagle medium supplemented with 10% fetal bovine serum (FBS; Gibco®-BRL, Carlsbad, CA, USA) and 100 U/ml penicillin-streptomycin (Solarbio, Beijing, China) at 37˚C in an incubator with 5% CO_2. The present study was approved by the ethics committee of Central South University (Changsha, Hunan, China).

Experimental design. Cells were seeded at 80-90% confluence in FBS-containing medium. HPMCs were cultured for 24 h in medium containing 5.6 mmol/l D-glucose and 10% FBS prior to being exposed to the various experimental conditions. To study the effect of different concentrations of glucose, the HPMCs were cultured in a medium containing 0, 30, 60 and 90 mmol/l D-glucose for 24 h. To study the effect of time, HPMCs were exposed to high glucose levels (60 mmol/l) for 0, 12, 24 and 48 h. Cells were then used for further analysis.

Immunofluorescence. Conditioned cells were grown on chamber slides. The cells were then washed twice with phosphate-buffered saline (PBS) and fixed with 2-4% paraformaldehyde for 15 min. Cells were permeabilized with 0.3% Triton X-100 (Beijing Dingguochangsheng Biotechnology Co., Ltd., Beijing, China) for 10 min and then blocked with 5% bovine serum albumin (Proliant Biologicals Inc., Ankeny, IA, USA) for 1 h. The primary antibodies, including mouse monoclonal anti-human vimentin antibody (Santa Cruz Biotechnology, Inc., Santa Cruz, CA, USA) and goat monoclonal anti-human E-cadherin antibody (Santa Cruz Biotechnology, Inc.) were incubated with the cells overnight at 4˚C. The cells were then incubated with secondary antibodies of fluorescein isothiocyanate-labeled rabbit anti-goat immunoglobulin G (IgG; 1:200; ZSGB-BIO, Beijing, China) and goat anti-mouse IgG (1:200; Zymed, San Francisco, CA, USA) for 1 h at room temperature. The cells were washed with PBS and 4',6-diamidino-2-phenylindole (Santa Cruz Biotechnology, Inc.) was used to stain the nuclei. Cells were then analyzed using a confocal microscope (Zeiss LSM 510; Carl Zeiss, Oberkochen, Germany).

Table I. Primer sequences used for qPCR.

Genes	Primer sequences
E-cadherin	5'-TCATGAGTGTCCCCCGGTAT-3'
	5'-TCTTGAAGCGATTGCCCCAT-3'
Vimentin	5'-GCTACGTGACTACGTCCACC-3'
	5'-TAGTTGGCGAAGCGGTCATT-3'
FN	5'-AACTGGTAACCCTTCCACACCC-3'
	5'-AGCTTCTTGTCCTACATTCGGC-3'
ILK	5'-CAACACGGAGAACGACCTCA-3'
	5'-GTGTCATCCCCACGGTTCAT-3'
GSK-3β	5'-GGAACTCCAACAAGGGAGCA-3'
	5'-TTCGGGGTCGGAAGACCTTA-3'
Cyclin D1	5'-GATGCCAACCTCCTCAACGA-3'
	5'-GGAAGCGGTCCAGGTAGTTC-3'
COL-1	5'-GCCAAGACGAAGACATCCCA-3'
	5'-GGCAGTTCTTGGTCTCGTCA-3'
GAPDH	5'-CAATGACCCCTTCATTGACC-3'
	5'-GACAAGCTTCCCGTTCTCAG-3'

qPCR, quantitative polymerase chain reaction; FN, fibronectin; ILK, integrin-linked kinase; GASK-3β, glycogen synthase kinase 3β; COL-1, collagen, type I.

Quantitative polymerase chain reaction (qPCR). Total RNA was extracted using an RNAiso Plus reagent (Takara Bio, Inc., Shiga, Japan), and cDNA was synthesized using a RevertAid™ First Strand cDNA Synthesis kit (MBI Fermentas, Amherst, NY, USA). qPCR was performed using an ABI PRISM® 7300 real-time PCR system (Applied Biosystems®, Carlsbad, CA, USA). Primers were based on human sequences, and the amplification efficiencies of all of the genes were similar. The primers used for qPCR are shown in Table I.

Western blot analysis. Total protein was extracted from HPMCs and separated using sodium dodecyl sulfate-polyacrylamide gel electrophoresis (Beijing Dingguochangsheng Biotechnology Co.). The polyvinylidene difluoride membrane (Millipore, Billerica, MA, USA) was blocked using 5% nonfat milk in Tris-buffered saline with 1% Tween 20 (Amresco Inc., Solon, Ohio, USA) for 2 h at room temperature. The membrane was subsequently incubated with the primary antibodies [mouse monoclonal anti-human vimentin, mouse monoclonal anti-human fibronectin (FN), goat monoclonal anti-human E-cadherin, rabbit polyclonal anti-human ILK, rabbit monoclonal anti-human p-GSK-3β, mouse monoclonal anti-human cyclin D1 and rabbit polyclonal anti-human collagen, type I (COL-1)] overnight at 4˚C, followed by incubation with horseradish peroxidase (HRP)-conjugated secondary antibodies (rabbit anti-goat, goat anti-rabbit and goat anti-mouse antibodies) for 1 h. The signals were detected using a Kodak

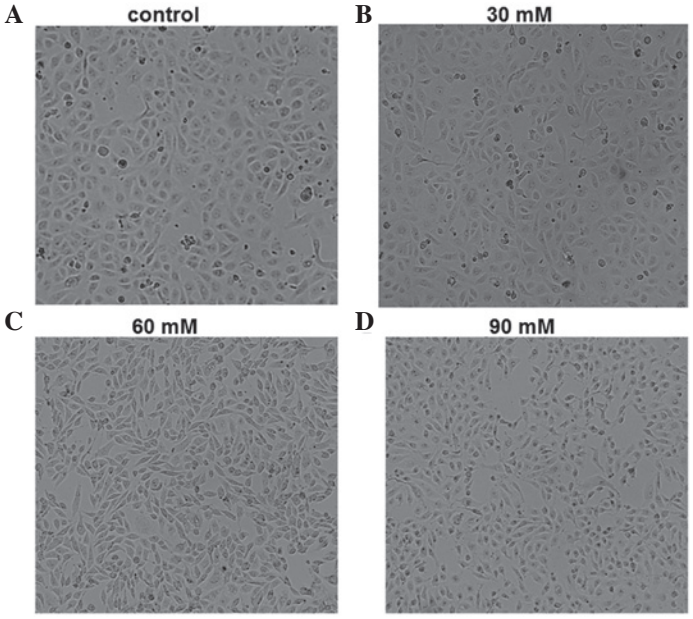

Figure 1. Morphological analysis of HPMCs cultured at high glucose levels. Cells were incubated with 30, 60 and 90 mM glucose for 24 h and observed under phase-contrast microscopy. (A) Control cells; (B-D) cells treated with (B) 30 mM glucose, (C) 60 mM glucose and (D) 90 mM glucose (magnification, x200). HMPCs, human peritoneal mesothelial cells.

Digital Imaging System (4000MM; Kodak, Rochester, NY, USA).

Small interfering RNA (siRNA) transfection. siRNA against ILK was purchased from Qiagen (Valencia, CA, USA) whilst negative control siRNA was purchased from Dharmacon (siGENOME® Non-Targeting siRNA #1; Thermo Fisher Scientific, Waltham, MA, USA). At 60% confluence, cells were washed with Opti-MEM® (Gibco®-BRL) and transfected with targeted or control siRNA (at a final concentration of 25 nM) in accordance with the manufacturer's instructions. Six hours post-transfection, Opti-MEM was replaced with normal medium and cells were further incubated for 24 or 48 h. The sequences of siRNA for ILK were as follows: 5'-CCUCUACAAUGUACUACAUTT dTdT and 3'-AUGUAGUACAUUGUAGAGGTT dGdT.

Statistical analysis. All of the data are expressed as the mean ± standard deviation and were analyzed by one-way analysis of variance using SPSS 13.0 statistical software (SPSS, Inc., Chicago, IL, USA). $P<0.05$ was considered to indicate a statistically significant difference.

Results

High glucose levels induce morphological changes in HPMCs. To determine the effect of high-glucose incubation on the morphology of HPMCs, cells were incubated with 30, 60 and 90 mM glucose for 24 h and observed using phase-contrast microscopy. Representative images are shown in Fig. 1. In the control group not treated with glucose, HPMCs were tightly packed with polygonal or oval morphology and were arranged in a paving stone-like manner. Following incubation with 30 mM glucose for 24 h, certain cells demonstrated an elongated morphology. However, following incubation with 60 mM glucose for 24 h, HPMCs exhibited a series of phenotypic changes compared with the control cells, including elongation, branching and loss of the paving stone appearance. The phenotypic changes were similar but more evident in cells incubated with 90 mM glucose compared with those incubated with 30 mM for 24 h. Therefore, cell morphology of HPMCs was markedly affected by glucose incubation, and these morphological changes were induced in a dose-dependent manner.

High glucose levels induce EMT in HPMCs. To investigate the effect of high-glucose incubation on peritoneal EMT, an *in vitro* EMT study was performed in HPMCs. In order to induce EMT in the HPMCs, cells were incubated with 60 mM glucose for 0, 12, 24 and 48 h, respectively. The markers for EMT were then analyzed using western blot analysis and qPCR. The detected markers included FN, COL-1, E-cadherin and vimentin. Representative results from the western blot analysis are shown in Fig. 2A. Following incubation for 24 h, the expression level of E-cadherin, an epithelial phenotype marker, was downregulated and reached the lowest level at 48 h. The expression level of vimentin, a mesenchymal marker, was almost undetectable at 0 h of incubation; however, expression was upregulated from as early as 12 h and peaked at 48 h. FN expression also increased from 12 h of incubation. COL-1 protein levels changed in a time-dependent manner, increasing from 12 h of incubation and peaking at 48 h of incubation. The representative qPCR results are shown in Fig. 2B. The qPCR results indicate that E-cadherin mRNA expression levels decreased in a time-dependent manner, and significant differences were observed at 24 h ($P<0.05$). FN mRNA expression levels increased in time-dependent manner. Significant differences were observed at 12 h ($P<0.05$). COL-1 and vimentin mRNA expression levels were both significantly increased at 12 h ($P<0.05$) and 24 h ($P<0.01$). These results suggest that incubation at high glucose levels increases the expression

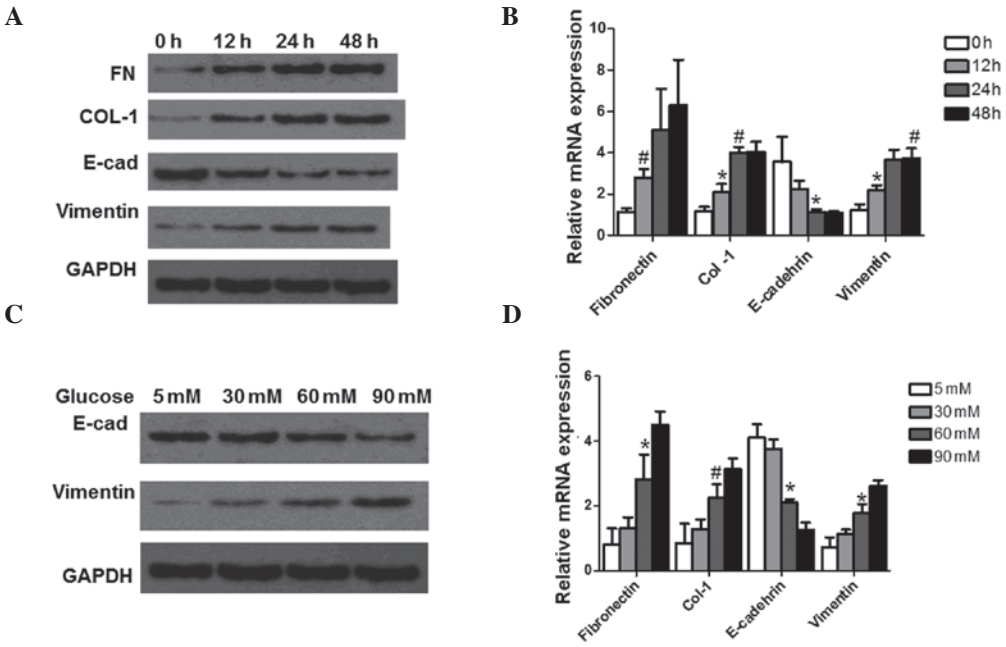

Figure 2. Expression analysis of EMT marker proteins at the protein and mRNA level following treatment with high levels of glucose. The analyzed proteins were FN, COL-1, E-cadherin and vimentin. GAPDH was used as an internal control. (A and B) Cells were incubated with 60 mM glucose for 0, 12, 24 and 48 h, respectively, prior to analysis. Representative results from the western blot analysis and qPCR are shown. (C and D) Cells were incubated with 5, 30, 60 and 90 mM glucose for 24 h prior to analysis. Representative results from the western blot analysis and qPCR are shown. Experiments were performed three times and data are expressed as the mean ± standard deviation. *P<0.05 and $^{\#}$P<0.01, compared with cells incubated for 0 h. EMT, epithelial to mesenchymal transition; FN, fibronectin; COL-1, collagen, type I; qPCR, quantitative polymerase chain reaction; E-cad, E-cadherin.

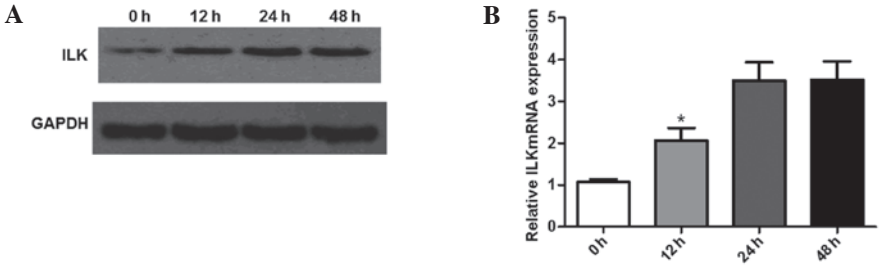

Figure 3. Analysis of ILK protein and mRNA expression levels following treatment with high levels of glucose. Cells were incubated with 60 mM glucose for 0, 12, 24 and 48 h prior to analysis. GAPDH was used as an internal control. Protein and mRNA expression levels of ILK were detected using (A) western blot analysis and (B) qPCR, respectively. The data are expressed as the mean ± standard deviation of three independent experiments. *P<0.05, compared with cells incubated for 0 h. ILK, integrin-linked kinase; qPCR, quantitative polymerase chain reaction.

of the ECM components and induces EMT in HPMCs in a time-dependent manner.

To further determine the effects of high glucose levels on peritoneal EMT, HPMCs were incubated in media containing 5, 30, 60 and 90 mM glucose for 24 h. The protein expression levels of E-cadherin and vimentin were analyzed using western blot analysis and the mRNA expression levels of FN, COL-1, E-cadherin and vimentin were determined using qPCR. Representative results from the western blot analysis are shown in Fig. 2C. Glucose treatment downregulated E-cadherin expression, with E-cadherin expression being lowest following treatment with 90 mM glucose. The expression of vimentin was almost undetectable following treatment with 5 mM glucose; however, expression increased following treatment with 30 and 60 mM glucose and peaked at 90 mM glucose. qPCR yielded similar results. As shown in Fig. 2D, mRNA expression levels of E-cadherin decreased in a dose-dependent manner and there was a significant decrease in expression levels following treatment with 60mM glucose compared with expression following treatment with 5 mM glucose (P<0.05). The mRNA expression levels of vimentin, COL-1 and FN also increased in a dose-dependent manner. Significant differences were observed at 60mM of treatment (P<0.05; P<0.01). These results suggest that expression of ECM components and the EMT of HPMCs were induced by glucose in dose-dependent manner.

ILK expression is increased during EMT in HPMCs. In order to examine the changes in ILK expression following incubation with glucose in HPMCs, western blot analysis and qPCR were performed. Prior to analysis, cells were incubated with 60 mM glucose for 0, 12, 24 and 48 h, respectively. As shown in Fig. 3A, ILK expression was upregulated in response to incubation at high glucose levels. The upregulation was observed from 12 h and peaked following 24 h of treatment. This was further confirmed by the results from the qPCR. As shown in Fig. 3B, ILK mRNA expression levels increased

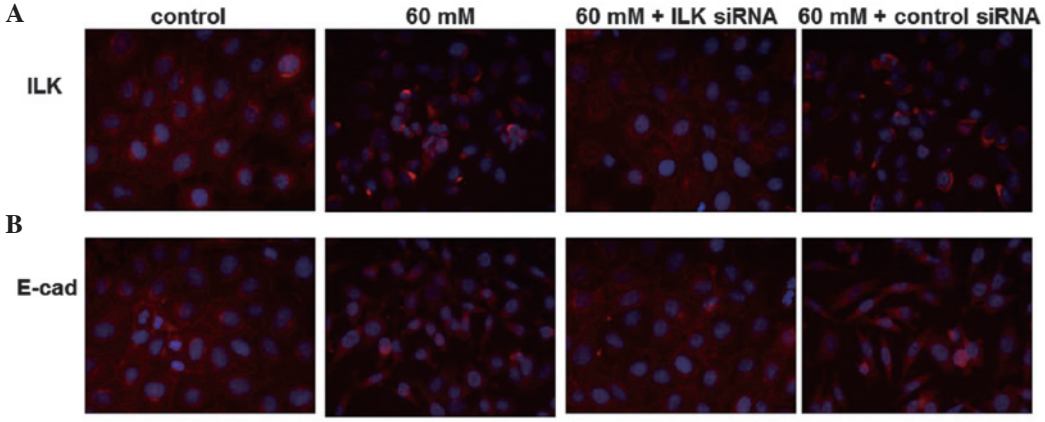

Figure 4. Immunofluorescence analysis of (A) ILK and (B) E-cadherin. ILK expression was knocked down using siRNA. Control cells and cells with ILK-knockdown were then treated with 60 mM glucose for 24 h prior to analysis. ILK, integrin-linked kinase; siRNA, small interfering RNA; E-cad, E-cadherin.

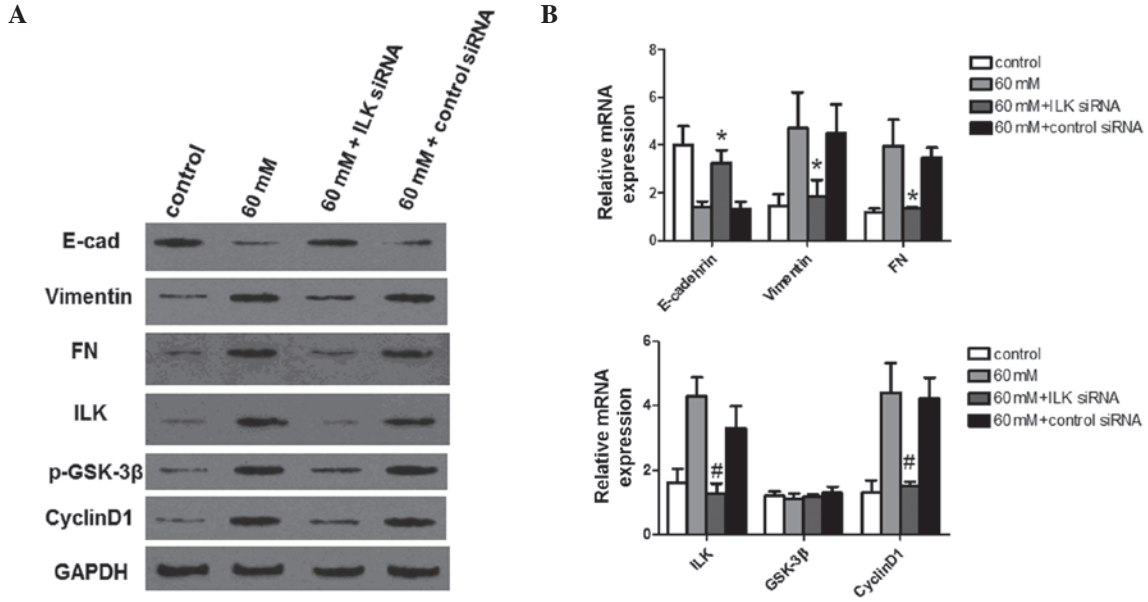

Figure 5. Expression analysis of EMT-associated proteins and downstream signal transduction proteins following ILK-knockdown. ILK expression was knocked down using siRNA. Control and ILK-knockdown cells were treated with 60 mM glucose for 24 h prior to analysis. E-cadherin, vimentin, FN, ILK, GSK-3β and cyclin D1 protein and mRNA expression levels were detected using (A) western blot analysis and (B) quantitative polymerase chain reaction, respectively. GAPDH was used as an internal control. Experiments were performed in triplicate and data are presented as the mean ± standard deviation. *P<0.05 and #P<0.01, compared with the cells treated with 60 mM glucose. EMT, epithelial to mesenchymal transition; ILK, integrin-linked kinase; siRNA, small interfering RNA; FN, fibronectin; GSK-3β, glycogen synthase kinase 3β; p-GSK-3β, phos-phorylated GSK-3β; E-cad, E-cadherin.

between 12 and 48 h of treatment. These results indicate that ILK expression was induced during EMT in HPMCs.

Distribution of ILK and E-cadherin in HPMCs induced by high glucose levels. In order to further elucidate the observed changes in ILK expression, the distribution of ILK in the normal HPMCs and during the development of fibrosis in the HPMCs was investigated using an immunofluorescence assay. Under normal glucose conditions, differentiated HPMCs exhibited a typical spreading cobblestone-like morphology with processes and expressed little ILK in the cytoplasm (Fig. 4A). In the HPMCs induced by high glucose levels (60 mM), however, a significant increase in ILK staining was observed, and the staining was equally distributed in the cytoplasm. HPMCs were then transfected with ILK-specific siRNAs to knock down ILK expression. In cells with ILK-knockdown, it was observed that ILK staining was abolished and the cells showed an epithelial morphology.

The distribution of E-cadherin in HPMCs was also observed using an immunofluorescence assay. As shown in Fig. 4B, strong staining for E-cadherin was visible in the plasma membrane of normal HPMCs. However, E-cadherin staining largely disappeared in the HPMCs induced by high glucose levels. By contrast, the E-cadherin staining markedly increased in response to ILK siRNA. In addition, the staining further confirmed the phenotypic transition of HPMCs from a spindle morphology with processes to a cobblestone appearance under high glucose conditions. This result further indicates that ILK was involved in HPMC EMT induced by high glucose levels.

Knockdown of ILK expression blocks EMT of HPMCs and suppresses high glucose-induced downstream signaling. To

further characterize the potential function of ILK in HPMCs, the effect of the knockdown of endogenous ILK on the expression levels of EMT-associated proteins and downstream signal transduction proteins were investigated. siRNA was used to knock down endogenous ILK expression. Protein and mRNA expression of E-cadherin, vimentin, FN, ILK, phosphorylated GSK-3β (p-GSK-3β) and cyclin D1 were detected using western blot analysis and qPCR, respectively. GAPDH was used as an internal control. The expression levels of EMT-associated proteins were first analyzed. As shown in Fig. 5A and B, transfection of HPMCs with specific siRNA resulted in a significant reduction in endogenous ILK expression at the protein and mRNA level, respectively ($P<0.01$). The results from the western blot analysis and the qPCR analysis demonstrated that knockdown of ILK significantly restored E-cadherin expression ($P<0.05$). However, downregulation of ILK significantly reduced vimentin and FN expression ($P<0.05$), preventing FN overproduction in response to stimulation by high glucose levels. These findings further show that EMT of HPMCs may be inhibited by ILK-knockdown.

GSK-3β is a known ILK downstream target. It was then investigated whether inhibition of ILK activity by siRNA leads to a reduction in GSK-3β phosphorylation induced by high glucose conditions. As shown in Fig. 5A, phosphorylation of GSK-3β induced by high glucose levels was inhibited by ILK-knockdown. However, the expression of GSK-3β at the mRNA level was not significantly affected (Fig. 5B), suggesting that ILK-knockdown by siRNA specifically blocks GSK-3β phosphorylation in HPMCs. Cyclin D1 is a key downstream target of activated canonical Wnt signaling. As demonstrated by the results from the western blot analysis and qPCR, cyclin D1 expression was also increased by high glucose treatment, but was significantly decreased following ILK-knockdown ($P<0.01$). In combination, these results suggest that ILK may inhibit EMT in HPMCs through phosphorylation of GSK-3β.

Discussion

In this study, high glucose levels were found to increase ILK expression in HPMCs. Under normal glucose conditions, HPMCs exhibited a spreading arborized morphology, whereas they had a cobblestone morphology under high glucose conditions. Furthermore, in the high-glucose environment, E-cadherin expression was found to be decreased, accompanied by an increased expression of the mesenchymal marker vimentin. These findings demonstrate that HPMCs underwent EMT in high glucose conditions.

It is known that ILK has a key role at the interface between the ECM, integrins, actin-based cytoskeleton and cellular phenotype in kidney diseases (27). In addition, ILK acts as an adaptor protein that interacts with nephrin and α-actinin-4 to form a ternary complex, which is essential for the maintenance of podocyte function and glomerular filter integrity (28). Previous studies have suggested that TGF-β1 and high glucose levels induce HPMCs to undergo EMT (1,2). Additionally, ILK inhibition with a small molecule inhibitor, QLT-0267, prevented EMT of podocytes and ameliorated proteinuria, suggesting that ILK was a key intracellular mediator in EMT. Of note, the inhibitor had no adverse effect on normal kidney structure and function (29). The disruption of the interaction between integrin and ILK may contribute to podocyte dysfunction, leading to EMT. In accordance with these results, in the present study it was demonstrated that high glucose levels induced ILK overexpression and EMT in HPMCs. Previous studies have demonstrated that particularly interesting new cysteine-histidine rich protein 1 (PINCH-1), an adaptor protein that interacts with ILK, is dysregulated in the fibrotic kidney following obstructive injury. The concomitant induction of PINCH-1 (30) and ILK (18) suggests that the PINCH-1-ILK complex may have a fundamental role in mediating tubular EMT. Tissue-type plasminogen activator (tPA) exerts its fibrogenic function by a novel signal transduction pathway. It binds to the membrane receptor low-density lipoprotein receptor-related protein 1 (LRP-1) and triggers the receptor tyrosine phosphorylation that, in turn, recruits β1 integrin and subsequently activates ILK signaling (31). ILK induction by TGF-β1 is clearly dependent upon intact Smad signaling in tubular epithelial cells, since overexpression of inhibitory Smad-7 abolishes Smad-2 phosphorylation and ILK induction. ILK signaling is also implicated in Snail expression. The kinase-dead form of ILK largely abolishes TGF-β1-induced tubular EMT and inhibition of ILK expression by hepatocyte growth factor (HGF), blocks tubular EMT and reduces renal fibrosis. ILK strategically bridges the integrins and actin cytoskeleton-associated proteins, including calponin homology domain-containing ILK binding protein and paxillin, and transmits signal exchanges between the intracellular and extracellular compartments (32-34). Consistently, a previous study also demonstrated that ILK induces an invasive phenotype in brain tumor cell lines via activator protein 1 (AP-1)-dependent upregulation of matrix metalloproteinase-9 (MMP-9) expression (35). Similarly, ILK directly phosphorylates GSK-3 on Ser 9, causing its inhibition, which leads to the stabilization of β-catenin and stimulation of the activity of AP-1 and cyclic adenosine monophosphate response element binding protein (20,36,37). Since GSK-3β is a downstream substrate for Akt, ILK also induces GSK-3β phosphorylation indirectly via the Akt pathway (14). The results of the present study found that the inhibition of ILK by siRNA inhibited ILK expression and attenuated EMT, suggesting that ILK is involved in the EMT of HPMCs, which is consistent with the results found in previous studies.

It has been reported that overexpression of active ILK in podocytes induces translocation of β-catenin to the cell nucleus, as well as nuclear colocalization of β-catenin with lymphoid enhancer-binding factor 1 (LEF-1) (38). In patients with primary focal segmental glomerulosclerosis (FSGS), the activation of ILK activated the Wnt signaling pathway and GSK-3β in damaged podocytes (37). The results of the present study showed that incubation of HPMCs at high glucose levels led to the acquisition of fibrotic characteristics and initiation of EMT. Additionally, high glucose conditions were demonstrated to upregulate ILK expression in a GSK-3β-dependent manner. In cultured podocytes, ILK has been shown to orchestrate a wide array of functions, including membrane proximal initiation of signal transduction via Akt, GSK-3β and β-catenin (15,16) and regulating cell phenotype and survival (15,16,39). A previous study demonstrated that

Dp71f modulates GSK3-β recruitment to the β1-integrin adhesion complex in PC12 cells (40).

Previous studies have shown that ILK inhibition blocks phosphorylated Akt (p-Akt), p-GSK-3β, β-catenin and Snail expression, as well as MMP9 and Twist expression (41). Changes in ECM composition may alter the balance between apoptosis and survival (42). ILK links the ECM with the intracellular compartment through interaction with the cytoplasmic domains of β1 and β3 integrins (43). As a central part of the ILK/PINCH/parvin complex, ILK connects the ECM with the actin cytoskeleton and transmits signals to the inner region of the cell through its serine/threonine kinase activity. The kinase activity of ILK is stimulated by integrins and soluble mediators, including growth factors and chemokines, and is regulated in a PI3K-dependent manner (44,45). EMT is mediated through several transcription repressors, including Snail, Slug, Twist, MMP-2, MMP-9 and zinc finger E-box-binding homeobox 1 (ZEB1), which induce EMT by suppressing the transcription of the E-cadherin gene, an epithelial cell marker and a potent suppressor of cell invasion and metastasis (46-48). Furthermore, it was demonstrated in the present study that downregulation of ILK also inhibits phosphorylation of GSK-3β in HPMCs. ILK regulates phosphorylation of its downstream targets Akt and GSK-3β on Ser 473 and Ser 9, respectively (49). GSK-3β, which is known as the 'guardian of the epithelial state', regulates Snail degradation through its phosphorylation on Ser 246. ILK and Akt are known to phosphorylate and inactivate GSK-3β, which in turn suppresses phosphorylation of Snail and leads to EMT (50,51). Maseki *et al* (52) demonstrated that EMT was mediated by activation of the Akt/GSK-3β/Snail pathway. Akt phosphorylates GSK-3β at Ser 9, leading to inactivation of its kinase activity. GSK-3β also interacts with ILK, and ILK phosphorylates GSK-3β at Ser 9 in an Akt-independent manner (53).

The phosphorylation of GSK-3β by ILK signaling pathways leads to the activation of transcription factors, including AP1 and the β-catenin/lymphocyte enhancer factor, which in turn stimulate MMP-9 and cyclin-D1, respectively (42). The results of the present study demonstrate that inhibition of ILK activity results in p-GSK-3β downregulation. Therefore, the results from the present study further confirm the previous findings, and suggest that ILK may have a crucial role in EMT through phosphorylation of GSK-3β. ILK overexpression in rat intestinal epithelial cells resulted in stimulation of the G1/S cyclin-Cdk complex and subsequent cell cycle progression (54). Furthermore, the dominant-negative mutant of ILK was shown to induce G1 cell cycle arrest in prostate cancer cells (55). This may indicate that the parallel cell cycle regulatory events seen in diseased podocytes (i.e., collapsing focal segmental glomerulosclerosis) may at least in part be downstream of ILK (56,57).

In conclusion, the results of the present study have demonstrate for the first time, to the best of our knowledge, that ILK has an important role in the high glucose level-induced EMT of HPMCs. Knockdown of ILK inhibits EMT of HPMCs, with an increase in E-cadherin and a decrease in vimentin expression levels. Furthermore, ILK-knockdown suppresses phosphorylation of GSK-3β, and thus inhibits its downstream pathway. Therefore, ILK, a newly identified peritoneal EMT regulator, may be used as a diagnostic marker for peritoneal fibrosis and may be a potential therapeutic target for the treatment of peritoneal fibrosis.

Acknowledgements

This study was supported by the 2010-2012 Key Projects for Clinical Disciplines of the Subordinate Hospital of the Ministry of Health.

References

1. Aroeira LS, Aguilera A, Selgas R, *et al*: Mesenchymal conversion of mesothelial cells as a mechanism responsible for high solute transport rate in peritoneal dialysis: role of vascular endothelial growth factor. Am J Kidney Dis 46: 938-948, 2005.
2. Yáñez-Mó M, Lara-Pezzi E, Selgas R, *et al*: Peritoneal dialysis and epithelial-to-mesenchymal transition of mesothelial cells. N Engl J Med 348: 403-413, 2003.
3. Kim YL: Update on mechanisms of ultrafiltration failure. Perit Dial Int 29 (Suppl 2): S123-S127, 2009.
4. Loureiro J, Aguilera A, Selgas R, *et al*: Blocking TGF-β1 protects the peritoneal membrane from dialysate-induced damage. J Am Soc Nephrol 22: 1682-1695, 2011.
5. Margetts PJ, Bonniaud P, Liu L, *et al*: Transient overexpression of TGF-{beta}1 induces epithelial mesenchymal transition in the rodent peritoneum. J Am Soc Nephrol 16: 425-436, 2005.
6. Vargha R, Endemann M, Kratochwill K, *et al*: Ex vivo reversal of in vivo transdifferentiation in mesothelial cells grown from peritoneal dialysate effluents. Nephrol Dial Transplant 21: 2943-2947, 2006.
7. Wang X, Nie J, Jia Z, *et al*: Impaired TGF-beta signalling enhances peritoneal inflammation induced by *E. coli* in rats. Nephrol Dial Transplant 25: 399-412, 2010.
8. Lee HB and Ha H: Mechanisms of epithelial-mesenchymal transition of peritoneal mesothelial cells during peritoneal dialysis. J Korean Med Sci 22: 943-945, 2007.
9. Zeisberg M and Duffield JS: Resolved: EMT produces fibroblasts in the kidney. J Am Soc Nephrol 21: 1247-1253, 2010.
10. Liu Y: New insights into epithelial-mesenchymal transition in kidney fibrosis. J Am Soc Nephrol 21: 212-222, 2010.
11. Hannigan GE, Leung-Hagesteijn C, Fitz-Gibbon L, Coppolino MG, Radeva G, Filmus J, Bell JC and Dedhar S: Regulation of cell adhesion and anchorage-dependent growth by a new beta 1-integrin-linked protein kinase. Nature 379: 91-96, 1996.
12. Legate KR, Montañez E, Kudlacek O and Fässler R: ILK, PINCH and parvin: the tIPP of integrin signaling. Nat Rev Mol Cell Biol 7: 20-31, 2006.
13. Dai HY, Zheng M, Lv LL, Tang RN, Ma KL, Liu D, Wu M and Liu BC: The roles of connective tissue growth factor and integrin-linked kinase in high glucose-induced phenotypic alterations of podocytes. J Cell Biochem 113: 293-301, 2012.
14. Li Y, Tan X, Dai C, Stolz DB, Wang D and Liu Y: Inhibition of integrin-linked kinase attenuates renal interstitial fibrosis. J Am Soc Nephrol 20: 1907-1918, 2009.
15. Teixeira Vde P, Blattner SM, Li M, *et al*: Functional consequences of integrin-linked kinase activation in podocyte damage. Kidney Int 67: 514-523, 2005.
16. Kretzler M, Teixeira VP, Unschuld PG, *et al*: Integrin-linked kinase as a candidate downstream effector in proteinuria. FASEB J 15: 1843-1845, 2001.
17. Guo L, Sanders PW, Woods A and Wu C: The distribution and regulation of integrin-linked kinase in normal and diabetic kidneys. Am J Pathol 159: 1735-1742, 2001.
18. Li Y, Yang J, Dai C, *et al*: Role for integrin-linked kinase in mediating tubular epithelial to mesenchymal transition and renal interstitial fibrogenesis. J Clin Invest 112: 503-516, 2003.
19. Persad S, Attwell S, Gray V, Mawji N, Deng JT, Leung D, *et al*: Regulation of protein kinase B/Akt-serine 473 phosphorylation by integrin-linked kinase: critical roles for kinaseactivity and amino acids arginine 211 and serine 343. J Biol Chem 276: 27462-27469, 2001.
20. Delcommenne M, Tan C, Gray V, Rue L, Woodgett J and Dedhar S: Phosphoinositide-3-OH kinase-dependent regulation of glycogen synthase kinase 3 and protein kinase B/AKT by the integrin-linked kinase. Proc Natl Acad Sci USA 95: 11211-11216, 1998.

21. Vi L, de Lasa C, DiGuglielmo GM, *et al*: Integrin-linked kinase is required for TGF-β1 induction of dermal myofibroblast differentiation. J Invest Dermatol 131: 586-593, 2011.
22. Li Y, Yang J, Luo JH, *et al*: Tubular epithelial cell dedifferentiation is driven by the helix-loop-helix transcriptional inhibitor Id1. J Am Soc Nephrol 18: 449-460, 2007.
23. Smeeton J, Zhang X, Bulus N, *et al*: Integrin-linked kinase regulates p38 MAPK-dependent cell cycle arrest in ureteric bud development. Development 137: 3233-3243, 2010.
24. Liu XC, Liu BC, Zhang XL, *et al*: Role of ERK1/2 and PI3-K in the regulation of CTGF-induced ILK expression in HK-2 cells. Clin Chim Acta 382: 89-94, 2007.
25. Stylianou E, Jenner LA, Davies M, Coles GA and Williams JD: Isolation, culture and characterization of human peritoneal mesothelial cells. Kidney Int 37: 1563-1570, 1990.
26. Rougier JP, Moullier P, Piedagnel R and Ronco PM: Hyperosmolality suppresses but TGF beta 1 increases MMP9 in human peritoneal mesothelial cells. Kidney Int 51: 337-347, 1997.
27. Blattner SM and Kretzler M: Integrin-linked kinase in renal disease: connecting cell-matrix interaction to the cytoskeleton. Curr Opin Nephrol Hypertens 14: 404-410, 2005.
28. Dai C, Stolz DB, Bastacky SI, St-Arnaud R, Wu C, Dedhar S and Liu Y: Essential role of integrin-linked kinase in podocyte biology: Bridging the integrin and slit diaphragm signaling. J Am Soc Nephrol 17: 2164-2175, 2006.
29. Kang YS, Li Y, Dai C, Kiss LP, Wu C and Liu Y: Inhibition of integrin-linked kinase blocks podocyte epithelial-mesenchymal transition and ameliorates proteinuria. Kidney Int 78: 363-373, 2010.
30. Li Y, Dai C, Wu C and Liu Y: PINCH-1 promotes tubular epithelial-to-mesenchymal transition by interacting with integrin-linked kinase. J Am Soc Nephrol 18: 2534-2543, 2007.
31. Hu K, Wu C, Mars WM and Liu Y: Tissue-type plasminogen activator promotes murine myofibroblast activation through LDL receptor-related protein 1-mediated integrin signaling. J Clin Invest 117: 3821-3832, 2007.
32. Guo L and Wu C: Regulation of fibronectin matrix deposition and cell proliferation by the PINCH-ILK-CH-ILKBP complex. FASEB J 16: 1298-1300, 2002.
33. Tu Y, Huang Y, Zhang Y, Hua Y and Wu C: A new focal adhesion protein that interacts with integrin-linked kinase and regulates cell adhesion and spreading. J Cell Biol 153: 585-598, 2001.
34. Nikolopoulos SN and Turner CE: Molecular dissection of actopaxin-integrin-linked kinase-Paxillin interactions and their role in subcellular localization. J Biol Chem 277: 1568-1575, 2002.
35. Troussard AA, Costello P, Yoganathan TN, Kumagai S, Roskelley CD and Dedhar S: The integrin linked kinase (ILK) induces an invasive phenotype via AP-1 transcription factor-dependent upregulation of matrix metalloproteinase 9 (MMP-9). Oncogene 19: 5444-5452, 2000.
36. D'Amico M, Hulit J, Amanatullah DF, *et al*: The integrin-linked kinase regulates the cyclin D1 gene through glycogen synthase kinase 3beta and cAMP-responsive element-binding protein-dependent pathways. J Biol Chem 275: 32649-32657, 2000.
37. Joshi MB, Ivanov D, Philippova M, Erne P and Resink TJ: Integrin-linked kinase is an essential mediator for T-cadherin-dependent signaling via Akt and GSK3beta in endothelial cells. FASEB J 21: 3083-3095, 2007.
38. Sellin JH, Umar S, Xiao J and Morris AP: Increased beta-catenin expression and nuclear translocation accompany cellular hyperproliferation in vivo. Cancer Res 61: 2899-2906, 2001.
39. Yang Y, Guo L, Blattner SM, Mundel P, Kretzler M and Wu C: Formation and phosphorylation of the PINCH-1-integrin linked kinase-alpha-parvin complex are important for regulation of renal glomerular podocyte adhesion, architecture, and survival. J Am Soc Nephrol 16: 1966-1976, 2005.
40. Cortés JC, Montalvo EA, Muñiz J, Mornet D, Garrido E, Centeno F and Cisneros B: Dp71f modulates GSK3-beta recruitment to the beta1-integrin adhesion complex. Neurochem Res 34: 438-444, 2009.
41. Kalra J, Sutherland BW, Stratford AL, *et al*: Suppression of Her2/neu expression through ILK inhibition is regulated by a pathway involving TWIST and YB-1. Oncogene 29: 6343-6356, 2010.
42. del Nogal M, Luengo A, Olmos G, Lasa M, Rodriguez-Puyol D, Rodriguez-Puyol M and Calleros L: Balance between apoptosis or survival induced by changes in extracellular-matrix composition in human mesangial cells: a key role for ILK-NfκB pathway. Apoptosis 17: 1261-1274, 2012.
43. Papachristou DJ, Gkretsi V, Rao UN, *et al*: Expression of integrin-linked kinase and its binding partners in chondrosarcoma: association with prognostic significance. Eur J Cancer 44: 2518-2525, 2008.
44. McDonald PC, Fielding AB and Dedhar S: Integrin-linked kinase - essential roles in physiology and cancer biology. J Cell Sci 121: 3121-3132, 2008.
45. Fielding AB, Dobreva I, McDonald PC, Foster LJ and Dedhar S: Integrin-linked kinase localizes to the centrosome and regulates mitotic spindle organization. J Cell Biol 180: 681-689, 2008.
46. Shin SY, Rath O, Zebisch A, Choo SM, Kolch W and Cho KH: Functional roles of multiple feedback loops in extracellular signal-regulated kinase and Wnt signaling pathways that reg-ulate epithelial-mesenchymal transition. Cancer Res 70: 6715-6724, 2010.
47. Acloque H, Thiery JP and Nieto MA: The physiology and pathology of the EMT. Meeting on the epithelial-mesenchymal transition. EMBO Rep 9: 322-326, 2008.
48. Xing Y, Qi J, Deng S, Wang C, Zhang L and Chen J: Small interfering RNA targeting ILK inhibits metastasis in human tongue cancer cells through repression of epithelial-to-mesenchymal transition. Exp Cell Res 319: 2058-2072, 2013.
49. McDonald PC, Oloumi A, Mills J, *et al*: Rictor and integrin-linked kinase interact and regulate Akt phosphorylation and cancer cell survival. Cancer Res 68: 1618-1624, 2008.
50. Doble BW and Woodgett JR: Role of glycogen synthase kinase-3 in cell fate and epithelial-mesenchymal transitions. Cells Tissues Organs 185: 73-84, 2007.
51. McPhee TR, McDonald PC, Oloumi A and Dedhar S: Integrin-linked kinase regulates E-cadherin expression through PARP-1. Dev Dyn 237: 2737-2747, 2008.
52. Maseki S, Ijichi K, Tanaka H, *et al*: Acquisition of EMT phenotype in the gefitinib-resistant cells of a head and neck squamous cell carcinoma cell line through Akt/GSK-3β/snail signalling pathway. Br J Cancer 106: 1196-1204, 2012.
53. Wu C and Dedhar S: Integrin-linked kinase (ILK) and its interactors: a new paradigm for the coupling of extracellular matrix to actin cytoskeleton and signaling complexes. J Cell Biol 155: 505-510, 2001.
54. Radeva G, Petrocelli T, Behrend E, Leung-Hagesteijn C, Filmus J, Slingerland J and Dedhar S: Overexpression of the integrin-linked kinase promotes anchorage-independent cell cycle progression. J Biol Chem 272: 13937-13944, 1997.
55. Tan C, Costello P, Sanghera J, Dominguez D, Baulida J, de Herreros AG and Dedhar S: Inhibition of integrin linked kinase (ILK) suppresses beta-catenin-Lef/Tcf-dependent transcription and expression of the E-cadherin repressor, snail, in APC-/- human colon carcinoma cells. Oncogene 20: 133-140, 2001.
56. Barisoni L, Mokrzycki M, Sablay L, Nagata M, Yamase H and Mundel P: Podocyte cell cycle regulation and proliferation in collapsing glomerulopathies. Kidney Int 58: 137-143, 2000.
57. Petermann AT, Pippin J, Hiromura K, *et al*: Mitotic cell cycle proteins increase in podocytes despite lack of proliferation. Kidney Int 63: 113-122, 2003.